Electroless copper plating obtained by Selective Metallisation using a Magnetic Field (SMMF)

Sofya Danilova , John E. Graves , Jordi Sort , Eva Pellicer , Gareth W.V. Cave , Andrew Cobley

PII: S0013-4686(21)01053-7
DOI: https://doi.org/10.1016/j.electacta.2021.138763
Reference: EA 138763

To appear in: *Electrochimica Acta*

Received date: 20 May 2021
Accepted date: 7 June 2021

Please cite this article as: Sofya Danilova , John E. Graves , Jordi Sort , Eva Pellicer , Gareth W.V. Cave , Andrew Cobley , Electroless copper plating obtained by Selective Metallisation using a Magnetic Field (SMMF), *Electrochimica Acta* (2021), doi: https://doi.org/10.1016/j.electacta.2021.138763

Electroless copper plating obtained by Selective Metallisation using a Magnetic Field (SMMF)

by Sofya Danilova[a], John E. Graves[a], Jordi Sort[b,c], Eva Pellicer[b], Gareth W.V. Cave[d], Andrew Cobley[a]

[a]Functional Materials Group, Coventry University, Priory St, Coventry CV1 5FB, UK;

[b]Departament de Física, Facultat de Ciències, Universitat Autònoma de Barcelona, E-08193 Bellaterra, Spain;

[c]Institució Catalana de Recerca i Estudis Avançats (ICREA), Pg. Lluis Companys 23, E-08010 Barcelona, Spain

[d]School of Science & Technology, Nottingham Trent University, Clifton Campus, Clifton, Nottingham NG11 8NS, UK

Corresponding author: Dr. Sofya Danilova; ad4398@coventry.ac.uk

Abstract

Lithography is the most commonly used method for the selective metallisation of non-conductive surfaces in the manufacture of electronic devices such as printed circuit boards and antennae. However, when used in subtractive mode, lithography results in the generation of large amounts of organic solvent and metal containing waste and requires high initial capital investment. For this reason, additive methods of selective metallisation are being widely investigated. In this work, a novel additive approach of Selective Metallisation using a Magnetic Field (SMMF) was studied. This method uses a magnetic catalyst to initiate the electroless plating process. Magnetic catalyst particles composed of magnetite-silicon dioxide-silver were synthesised by a wet-chemical procedure. Their composition was analysed by scanning electron microscopy and energy dispersive X-ray spectroscopy and the phase formation was confirmed by X-ray diffractometry. Catalytic activity towards formaldehyde oxidation and the magnetic properties of particles were confirmed by cyclic voltammetry and vibrating sample magnetometry, respectively. The results showed that the particles can be used as a catalyst for electroless copper plating and are attracted by the magnetic field. The pattern of deposition of the magnetic catalyst is defined by the magnetic field. Two different configurations of magnet and substrate were used to deposit the catalyst dispersion onto the substrate surface. In both cases, the particles were attracted by the magnetic field and deposited exclusively where the magnetic field was applied. Subsequent electroless copper plating also only occurred at these areas. Parallel lines of electroless copper were obtained. The effect of the magnetic field on magnetic catalyst deposition and subsequent electroless plating was studied and key process-specific defects were identified.

Keywords: catalyst particles; copper plating; electroless deposition; magnetic particles; selective metallization.

Introduction

Selective metallisation of non-conductive materials is a manufacturing process employed in the fabrication of electronic devices such as printed circuit boards (PCBs) and antennae. Conductive metal tracks are required to transfer an electric signal from one part of a device to another and can be created on non-conductive material by either subtractive or additive approaches. Lithography is the most commonly used method of conductive track creation and uses the subtractive approach, in which the whole substrate surface is metallised and tracks are created via the selective etching of metal. It is a mature technology which enables creation of high-quality conductive tracks, although it also results in generation of waste e.g. organic solvents and removed copper. Although there are number of approaches that can be used to reduce or recycle this waste, there is no universal system to eliminate it. While recycling systems are available, they are however, costly and labour-intensive [1].

In the additive approach, metal is deposited directly onto the substrate in the required pattern, which results in lower levels of metal waste than the subtractive technique. Often the metal is deposited using the electroless plating process, an inexpensive method of substrate metallisation which is frequently used in PCB and antenna manufacturing [2]. Electroless plating of non-conductive materials requires prior deposition of a catalyst (usually palladium [3–5], but other noble metals can also be used [6–9]) onto the substrate surface. Subsequent electroless plating results in metal deposition onto the activated surface. Some additive selective metallisation techniques are based on selective catalysation of the surface and result in specific electroless metal deposition exclusively at the catalysed areas. Selective catalysation can be achieved by microcontact printing [10,11], ink-jet

printing [12–15], or laser activation of the surface [16–19]. Although some techniques have found applications in electronics manufacturing, none of them have been able to completely replace the lithography process. Therefore, there is still an unmet demand for additive metallisation techniques which can compete with and potentially replace the lithography process.

The catalyst for electroless plating can be deposited from a dispersion of nanoparticles. Selective deposition of nanoparticles can be achieved via application of a magnetic field. This has been demonstrated using magnetite nanoparticles and is often used in bioscience [20–23]. The magnetic "pattern" is created by a magnetic array, a steel template and superposition of magnets. The ferromagnetic nanoparticles are attracted to the areas with the highest magnetic flux density (B), to form a desired pattern on the substrate surface.

Selective metallisation using a magnetic field (SMMF) is a novel approach of additive selective electroless plating which uses a magnetic field to direct the catalyst nanoparticles onto the substrate surface in a desired pattern (Figure 1). Instead of an expensive precious metal palladium catalyst, a magnetic magnetite-silver composite catalyst was used. Although the SMMF method is at an early stage of development, previous work by our group has demonstrated the ability to achieve a selective pattern of parallel lines by using a magnet [24–26] .

Figure 1.

The aim of the present work is to study the effect of the magnetic field on the deposition of the catalyst and the subsequent electroless copper plating. Unlike commonly used catalysts such as palladium, the magnetic catalyst in the SMMF process deposits due to the attractive

forces of the magnetic field. This leads to various process-specific cases of catalyst arrangement, which can be used to guide electroless plating.

2. Experimental

The water used in all experiments was purified by the process of reverse osmosis and is referred to in the text as RO water.

2.1 Synthesis of magnetic nanoparticles catalyst

Nanoparticle synthesis was based on the procedure explained elsewhere [27], with slight modifications. Magnetite was synthesised by the precipitation method. A solution of 25% ammonium hydroxide (20 ml) (Sigma Aldrich) was added dropwise to a 400 ml 0.01 M iron sulphate heptahydrate solution (Fisher Scientific) and the mixture was stirred for 1 h at 20 ± 1 ^{o}C. Then the synthesised particles were washed with water 3 times and dried at 50 ^{o}C for 16 h. Dry magnetite nanoparticles (0.05 g) were dispersed by ultrasonication in 100 ml methanol (Extra Pure, Fisher Chemical). Then the synthesis procedure from the original paper was followed. The synthesised magnetite nanoparticles (0.05 g) were dispersed in a mixture of 100 ml methanol (Extra Pure, Fisher Chemical) and 10 ml 25% ammonium hydroxide by ultrasonication for 10 min. Then 0.02 ml of tetraethyl orthosilicate (98%, ACROS Organics) was added. The dispersion was ultrasonicated for 2 h. The obtained particles were separated using a magnet and washed in methanol 3 times. The separated particles were then dispersed in 50 ml solution of 0.01 M hydrochloric acid and 0.6 g tin chloride (both Fisher Chemical) for 30 min. After that, the particles were again separated using a magnet and washed in RO water 3 times. The separated particles were dispersed in 50 ml 0.13 M ammoniacal silver nitrate by ultrasonication for 1 h. Tollens reagent was

freshly prepared before use. Silver nitrate (1.1 g) was dissolved in 10 ml of RO water. Ammonium hydroxide (25 %) was added dropwise to silver nitrate solution and stirred vigorously until the formed brown precipitate dissolved completely. Then, 5 ml of sodium hydroxide solution (3%) was added and followed by dropwise addition of the ammonium hydroxide to dissolve the precipitate until clear. In short, as proposed by the authors of the original work, the magnetite particles were then consecutively covered by layers of silicon dioxide, tin and silver. The obtained particles were magnetically separated, washed in reverse osmosis (RO) water and dried overnight at 50 ^{o}C.

2.2 Dispersion preparation

Magnetic catalyst particles (0.25 g) were dispersed by ultrasonication in 100 ml RO water for 30 min. A Langford 575 ultrasonication cleaning unit was used to perform ultrasonication, operating at frequency of 40 Hz and power of 1.4 W per 100 ml of water according to the calorimetry measurements. The obtained dispersion was either immediately used as a catalyst as obtained or used after filtration with QL 120 (pore size 6 µm) filter paper (Fisher Scientific).

2.3 Magnetic template preparation

Two configurations were used in the study. **Configuration 1** (Figure 2, A) consists of a single neodymium iron boron N42 permanent magnet with dimensions 10 x 5 x 2 mm^3, attached by north or south pole to the 3 mm plastic substrate by tape.

Configuration 2 (Figure 2, B) consists of a 0.41 mm thick non-conductive substrate, steel template and a magnet. The substrate was pre-treated by the swell-and-etch approach. The substrate was first placed in ethylene glycol at 80 ^{o}C for 10 min (swell), then it was placed in

a potassium permanganate (75 g/l) and sodium hydroxide (40 g/l) mixture for 20 min at 80 ^{o}C (etch). At the end, the substrate was washed in a 3 vol% mixture of sulfuric acid (98 %) and hydrogen peroxide (37 %) to neutralize potassium permanganate residues.

A steel template consisting of 16 parallel lines (0.5 mm thick, with distance between lines of 0.75 mm) was placed behind the substrate. Behind the steel template a neodymium iron boron N42 magnet with dimensions 20 x 20 x 10 mm^3 was affixed by either its north or south pole.

Figure 2.

2.4 Selective metallisation using a magnetic field

Electroless plating chemistry was supplied by AGAS Electronic Materials. First, the substrate was pre-treated with 10 vol% Circuposit Conditioner 3320A for 5 min at 46 ^{o}C. Then, the substrate was rinsed in RO water for 5 min. After the substrate was arranged in either magnetic configuration 1 or configuration 2, it was placed in the catalyst dispersion. The catalyst was deposited for 30 s unless otherwise specified.

Next, the substrate was gently rinsed in RO water and placed in the electroless plating bath. A Circuposit 3350-1 electroless copper plating bath was used, which operates at a basic pH and uses formaldehyde as a reducing agent. The deposition was conducted for 25 min at 46 ^{o}C. After, the substrate was rinsed in RO water and dried in air.

2.5 Characterisation

A Sigma 500 VP scanning electron microscope (SEM) with an X-MaxN 80 Oxford Instruments silicon drift detector fitted (EDX) were used to map the element distribution of magnetic

catalyst particles and image the deposited catalyst and electroless copper on the non-conductive substrate. The SEM was operated by using a secondary electron (SE2) detector.

The crystal structure of the nanoparticles was confirmed using a PANalytical X-Ray Diffractometer. The measurement angle (2Θ) was from 10^{o} to 80^{o}. The scan was collected using a step of 0.02^{o}. The magnetic properties of the catalyst nanoparticles were evaluated using a MicroSense Vibrating Sample magnetometer.

The composition of catalyst particles was analysed by an Optima 8300 PerkinElmer optical emission spectroscope. The particles (0.002 g) were dissolved in 10 ml of concentrated nitric acid (70 %), ACS grade and after, samples were diluted in RO water for analysis.

The catalytic activity of the particles was confirmed by cyclic voltammetry, which was performed using an analytic radiometer PST050, VoltaLab potentiostat. The particles (0.005 g) were dispersed in 1.5 ml of water by ultrasonication and then 5 µl was drop-coated onto the vitreous (or 'glassy') carbon electrode with a surface area of 0.07 cm^2. A three-electrode system was used and consisted of a working electrode (modified vitreous carbon), reference electrode (Ag/AgCl) and counter electrode – platinum sheet 1 cm^2. The measurements were performed in the following water-based electrolytes: 1) 0.2 M sodium hydroxide; 2) 0.2 M sodium hydroxide with 0.1 M formaldehyde. Measurement were performed at room temperature with a sweep rate of 50 mV/s.

Finite Element Method Magnetics (FEMM) software was used for modelling of the magnetic flux density distribution across the sample surface.

Adhesion was tested by using a tape test in accordance with ASTM D3359 standards. Because the sample was selectively metallised, the surface was not cut. Pressure sensitive tape was applied on the sample surface for 5 min and then removed.

3. Results

3.1 Magnetic catalyst

The structure of the obtained composite nanoparticles was confirmed by XRD analysis (Figure 3). The XRD spectrum confirmed the formation of both a cubic spinel structure of magnetite (PDF code Fe_3O_4: 01-088-0315) and face-centered cubic silver (PDF Code Ag: 01-087-0717) phases.

Figure 3.

The distribution of the elements across the sample was mapped by SEM/EDX analysis (Figure 4). These analyses revealed that both iron and silver were spread across the analysed particles, which confirmed composite formation. This is in agreement with the results reported by the original authors of the synthesis procedure [27].

Figure 4.

In the present study, it was important to characterise the magnetic and catalytic properties of the synthesised composite, which had not been previously reported. The ferrimagnetic properties of the particles were confirmed by VSM analysis (Figure 5, A). The obtained magnetization curve had a characteristic shape commonly observed in soft ferromagnetic or

ferrimagnetic materials. This confirmed that the particles can be attracted by the magnet. The composite nanoparticles had lower magnetization values compared to bare magnetite particles, due to the presence of paramagnetic elements in composite structure – silver and silicon dioxide. The magnetization values were also comparable with those reported previously in nanoparticles of similar composition obtained by other methods [28,29]. Particles in the current work had similar magnetization values to those seen in our previous work [26] and are expected to perform similarly during SMMF deposition.

Figure 5.

The catalytic properties of the composite particles were evaluated by cyclic voltammetry – a technique commonly used to confirm the catalytic activity of material in the electroless plating reaction. The process of electroless copper plating can be understood as two interdependent chemical reactions: formaldehyde oxidation (the anodic reaction (1)) and copper reduction (the cathodic reaction (2)) [30]:

Reaction	**E^o vs SHE (V)**	
$2HCHO + 4OH^- \rightarrow 2HCOO^- + H_2 + 2H_2O + 2e^-$	0.32 (pH 12)	(1)
$Cu(EDTA)^{2-} + 2e^- \rightarrow Cu^0 + EDTA^{4-}$	-0.216	(2)

Electrons released during formaldehyde oxidation are involved in the following copper reduction reaction. This means that kinetically, formaldehyde oxidation is the rate limiting step of the electroless plating process. Due to the specific bath formulation for electroless plating, the formaldehyde oxidation reaction does not happen spontaneously in solution but must be initiated by a catalyst - usually a noble metal. The ability of the metal to catalyse formaldehyde oxidation can be measured by cyclic voltammetry, which involves placing the catalyst and reducing agent in contact, and monitoring electron transfer at a range of potentials. In this experiment, increased electron transfer indicates that the reaction of

formaldehyde oxidation is occurring, while low electron transfer means that the metal cannot catalyse the anodic reaction. The recorded peak of electron transfer is characteristic for each metal, and for Ag is usually observed at 0-100 mV vs Ag/AgCl electrode [31–33]. Figure 5, B shows that in a solution of sodium hydroxide alone, no change in current was registered, which indicated that no redox reaction occurred on the catalyst surface. This means that there were no electrochemical processes which could hinder the recording of formaldehyde oxidation. After addition of formaldehyde, an oxidation current was registered with a peak at 100 mV, demonstrating that formaldehyde oxidation occurred on the composite particles. This means that the magnetic catalyst particles can initiate formaldehyde oxidation and, therefore, can potentially be used to initiate the electroless copper plating reaction. Because magnetite does not usually show catalytic properties for formaldehyde oxidation, it was important for the current work to confirm that composite particles of magnetite and silver will still exhibit catalytical properties that are typical for silver but not for magnetite.

In summary, the composite particles obtained in the present work were ferromagnetic and catalytic toward the electroless copper plating process and can potentially be used for the SMMF process.

3.2 Deposition with single magnet

Synthesised magnetic catalyst particles were dispersed by ultrasonication in water . Then the particles were deposited onto the non-conductive substrate using configuration 1 (Figure 2, A), in which a single magnet was placed behind the substrate. Due to the magnetic nature of particles demonstrated above, the particles were attracted to the surface of the substrate at the area with the highest magnetic field influence. The particles remained on

the surface due to magnetic interaction between particles and the magnet, which was placed behind the substrate. The SEM image of the substrate with deposited catalyst (Figure 6, A) shows the presence of agglomerates with a diameter of 5 μm and higher. The size of the catalyst particles can significantly influence the quality of the subsequent deposit and can affect the smoothness of deposited copper – the larger the particles the rougher the plating is obtained [34]. Therefore, it was essential to eliminate particularly large agglomerates from the dispersion. This was accomplished by filtration (using filers with 5 μm pores sizes). As a result, only small (below 5 μm) particles and agglomerates were present in dispersion and were subsequently deposited onto the substrate surface. To further improve the process, catalyst particles with a more uniform size should be tested in future work.

Figure 6.

The composition of the dispersion was analysed by ICP (Figure 6, C). The analysis showed that the metal (iron and silver) concentration in the dispersion decreased after filtration from 135 mg/L to 108 mg/L. The proportion of iron to silver remained constant at 58:42 before and after filtration, which means that filtered agglomerates also had a composite structure and were not composed predominantly of silver or magnetite.

Electroless copper plating was performed after the catalyst was deposited onto the substrate. Distinctive copper deposition was obtained at the edges of the pattern (Figure 7, A). According to the SEM image, the copper grows in a needle-like shape (Figure 7, B) with the needles oriented in the same direction as the magnetic field lines. The length and diameter of needles varies across the sample from 3 to 30 μm and 1 to 10 μm respectively. Such a large size distribution is possibly due to the difference in the magnetic field strength

across the substrate surface. Copper is a diamagnetic material [35] that does not align in the magnetic field during deposition and growth. The growth alignment may have been caused by the arrangement of the catalyst particles parallel to the magnetic field lines which often happens when magnetic particles deposit onto the surface [36,37].

Figure 7.

Copper also deposited at the centre of the pattern as seen in Figure 7, A. The deposit and catalyst were removed by blowing compressed air onto the sample. This indicated poor adhesion of the copper to the substrate at the centre of the pattern. This occurred due to the overloading of the substrate with catalyst. The attraction of the magnetic particles is proportional to the magnetic flux density (B) [38]. Its distribution, depicted in Figure 8, shows that the B was the highest at the centre of the pattern and therefore more of the catalyst was attracted to the centre. Equal distribution of the catalyst along the substrate surface can be achieved by modifying the pattern of the magnetic field on the substrate surface. Several works have shown that equal flux density can be achieved in repetitive simple patterns [23,38], suggesting that more complex patterns may also be possible.

Figure 8.

Different possible cases of catalyst and subsequent copper deposition are depicted schematically in Figure 9. Case 1 shows desirable catalyst distribution which is spread uniformly across the substrate surface, which results in uniform copper growth. Case 2 shows the needle-like arrangement of catalyst on the surface, which is caused by the tendency of magnetic particles to align with magnetic field lines. Subsequent copper deposition then follows the needle-like arrangement of the catalyst and results in the needle-like copper growth. At the centre of the substrate the catalyst was deposited as

depicted in case 3. At the higher catalyst concentration, the magnetic catalyst particles form 3D structures on the substrate surface [22]. Subsequent copper plating did not occur on the substrate surface itself and only covered the catalyst particles, as schematically depicted in Figure 9 (case 3). The catalyst did not have any adhesion to the substrate, which resulted in poor adhesion of deposited copper. In our previous work [24] , that effect was not observed due to the use of a lower concentration of catalyst in the dispersion, which resulted in less catalyst deposited at the centre of the pattern (case 1).

Figure 9.

3.3 Deposition with a template

A template consisting of parallel steel plates was used in order to demonstrate the ability of the SMMF process to deposit copper in a predefined pattern. The effects of the template on the magnetic flux density is shown in Figure 10. B rises in the areas which overlay the template fins and decreases between them. An edge effect was also observed in the simulation, which is due to the nature of the magnetic field distribution [39].

Figure 10.

SEM images of catalyst deposited on the substrate using the magnetic template are shown in Figure 11. The substrate was immersed in the catalyst solution for 15, 30 or 60 s. According to Figure 10, longer immersion resulted in a more defined electroless copper plating. Catalyst deposition for 15 s and subsequent electroless deposition did not result in any copper plating. It is clear from the SEM image that the catalyst does not continuously cover the surface of the substrate and many gaps remain between particles on the surface (Figure 11, A).

Figure 11.

When the catalyst was deposited for either 30 or 60 s, the substrate surface was completely covered by catalyst (Figure 11, B, C), although more copper plating was obtained after surface catalysation for 60 s (cf. Figure 11, E, F). SEM images of the deposited catalyst did not reveal significant differences in the coverage of the substrate surface by catalyst between these samples. The difference in resultant copper plating between these samples may be due to differing amounts of catalyst deposited. Longer exposure to the catalyst solution lead to an increased amount of catalyst in the 60 s sample and therefore more active catalyst sites, which initiated the electroless copper plating. The increase in catalyst sites also lead to more continuous copper plating (Figure 11, H).

A difference in the quality of the plated copper was observed between lines within the same sample (Figure 12, A). The lines located closer to the edge of the sample have copper deposited mainly at the line edge (Figure 12, B-D), while within the rest of the line non-continuous islands of copper were formed. This is identical to the results of deposition with a single magnet – higher attraction at the centre of the line lead to overloading of the area with catalyst which was later removed due to low adhesion to the substrate (Figure 9, case 3).

Figure 12.

In configuration 2 (Figure 2, B), lines located closer to the centre of the pattern have more copper remaining, though 3D needle-like structures were formed (Figure 9, case 2) due to the arrangement of catalyst parallel to the magnetic field lines (Figure 12, E, F). At the centre of the pattern, continuous copper lines were obtained (Figure 12, G). In this case, lower attractive forces lead to less catalyst attraction which resulted in the optimal amount of catalyst deposition required for electroless copper plating (Figure 9, case 1).

The resistance of the deposit was tested by multimeter at the area of smooth deposit. The resistance was 0.8 Ohm/cm. No conductivity was measured at the area with needle-like deposits, which confirmed that continuous film was not formed in those regions and suggesting that these defects should be eliminated in order to obtain a conductive layer of copper.

The results of adhesion testing are presented in Figure 13. The sample was evaluated by SEM after the tape test. The area of deposit in which needle formation was absent was not affected by tape removal (Figure 13, A, B), however the region with needles was significantly changed after the tape test – many needles were removed, indicating low adhesion to the substrate (Figure 13, C, D). This highlighted the necessity to eliminate needle-like formation in order to achieve a copper film deposited in a continuous layer.

Overall, the results indicate that the variation in the B around the sample lead to differences in the electroless copper plating quality, though these were not observed at the catalyst deposition stage. Further investigation into the process of catalyst deposition in the magnetic field will lead to a greater understanding of the SMMF process and will help improve the quality of the deposited copper.

4. Conclusion

This work demonstrated the novel approach of selective metallisation of non-conductive material using a magnetic field – the SMMF process. The magnetic templates were used to direct magnetic catalyst deposition onto a non-conductive substrate. This catalyst initiated the electroless copper plating process. Parallel copper lines with a width of 300 µm and a resistance of 0.8 Ohm/cm were deposited using the SMMF process.

The unique distribution of catalyst that resulted from using a magnetic field for deposition and the effect of this distribution on the subsequent electroless copper plating process were studied. The following key findings were made:

- The magnetic catalyst tends to arrange parallel to the magnetic field lines which can result in needle-like electroless copper plating.
- Excessive catalyst deposition caused by higher strength magnetic fields can lead to overpopulation of the substrate surface with catalyst and result in low adhesion of the deposited copper.

Obtaining a catalyst with a narrower size distribution as well as improving the template for the magnetic field configuration should be the main objectives of future work. This will help improve the SMMF process and allow for demonstration of the potential of the process in industrial applications.

Acknowledgements

The authors want to acknowledge Coventry University, which sponsored the present research and also COST MP1407 which sponsored the collaboration with Autonomous University of Barcelona Universitat Autònoma de Barcelona. Partial financial support by the European Research Council (SPIN-PORICS 2014-Consolidator Grant, Agreement Nº 648454), the Catalan Government (2017-SGR-292) and the Spanish Government (MAT2017-86357-C3-1-R) is also acknowledged.

Declaration of interests

The authors declare that they have no known competing financial interests or personal relationships that could have appeared to influence the work reported in this paper.

References

[1] J. Coombs, F. Clyde, Printed circuits handbook, McGraw-Hill Education, 2008.

[2] V.M. Dubin, Y. Shacham-Diamand, B. Zhoo, P.K. Vasudev, C.H. Ting, Selective and blanket electroless copper deposition for ultralarge scale integration, J. Electrochem. Soc. 144 (1997) 898–908. https://doi.org/10.1149/1.1837505.

[3] G. Mallory, Electroless Plating: Fundamentals and Applications, AESF, 1991.

[4] E. Matijević, A.M. Poskanzer, P. Zuman, The Characterization of the Stannous Chloride/ Palladium Chloride Catalysts for Electroless Plating, NASF Surf. Technol. White Pap. 61 (2016) 958–965.

[5] X. Cui, D.A. Hutt, D.J. Scurr, P.P. Conway, The evolution of Pd/Sn catalytic surfaces in electroless copper deposition, J. Electrochem. Soc. 158 (2011) 172–177. https://doi.org/10.1149/1.3536543.

[6] C.-C. Yang, Y.-Y. Wang, C.-C. Wan, Synthesis and Characterization of PVP Stabilized Ag/Pd Nanoparticles and Its Potential as an Activator for Electroless Copper Deposition, J. Electrochem. Soc. 152 (2005) C96. https://doi.org/10.1149/1.1850379.

[7] C.C. Yang, C.C. Wan, Y.Y. Wang, Synthesis of Ag/Pd nanoparticles via reactive micelles as templates and its application to electroless copper deposition, J. Colloid Interface Sci. 279 (2004) 433–439. https://doi.org/10.1016/j.jcis.2004.06.098.

[8] J.-L. Lan, C.-C. Wan, Y.-Y. Wang, Mechanistic Study of Ag/Pd-PVP Nanoparticles and Their Functions as Catalyst for Electroless Copper Deposition, J. Electrochem. Soc. 155 (2008) K77–K83. https://doi.org/10.1149/1.2838908.

[9] C.L. Lee, Y.L. Tsai, C.W. Chen, Specific and mass activity of silver nanocube and nanoparticle-based catalysts for electroless copper deposition, Electrochim. Acta. 104 (2013) 185–190. https://doi.org/10.1016/j.electacta.2013.04.116.

[10] S.C. Huang, T.C. Tsao, L.J. Chen, Selective electroless copper plating on poly(ethylene terephthalate) surfaces by microcontact printing, J. Electrochem. Soc. 157 (2010) 222–227. https://doi.org/10.1149/1.3306136.

[11] P.C. Hidber, W. Helbig, E. Kim, G.M. Whitesides, Microcontact Printing of Palladium Colloids: Micron-Scale Patterning by Electroless Deposition of Copper, Langmuir. 12 (1996) 1375–1380. https://doi.org/10.1021/la9507500.

[12] C.C. Tseng, Y.H. Lin, Y.Y. Shu, C.J. Chen, M. Der Ger, Synthesis of vinyl acetate/Pd nanocomposites as activator ink for ink-jet printing technology and electroless copper plating, J. Taiwan Inst. Chem. Eng. 42 (2011) 989–995. https://doi.org/10.1016/j.jtice.2011.05.002.

[13] B.K. Park, D. Kim, S. Jeong, J. Moon, J.S. Kim, Direct writing of copper conductive patterns by ink-jet printing, Thin Solid Films. 515 (2007) 7706–7711. https://doi.org/10.1016/j.tsf.2006.11.142.

[14] C.-Y. Kao, K.-S. Chou, Electroless Copper Plating onto Printed Lines of Nanosized Silver Seeds, Electrochem. Solid-State Lett. 10 (2007) D32. https://doi.org/10.1149/1.2431241.

[15] Y. Wang, Y. Wang, J. ju Chen, H. Guo, K. Liang, K. Marcus, Q. ling Peng, J. Zhang, Z. sheng Feng, A facile process combined with inkjet printing, surface modification and electroless deposition to fabricate adhesion-enhanced copper patterns on flexible polymer substrates for functional flexible electronics, Electrochim. Acta. 218 (2016) 24–31. https://doi.org/10.1016/j.electacta.2016.08.143.

[16] J. Xu, Y. Liao, H. Zeng, Z. Zhou, H. Sun, J. Song, X. Wang, Y. Cheng, Z. Xu, K. Sugioka, K. Midorikawa, Selective metallization on insulator surfaces with femtosecond laser pulses, Opt. Express. 15 (2007) 12743. https://doi.org/10.1364/oe.15.012743.
[17] N.S. Dellas, K. Meinert, S.E. Mohney, Laser-enhanced electroless plating of silver seed layers for selective electroless copper deposition, J. Laser Appl. 20 (2008) 218–223. https://doi.org/10.2351/1.2995767.
[18] H.S. Cole, Y.S. Liu, J.W. Rose, R. Guida, Laser-induced selective copper deposition on polyimide, Appl. Phys. Lett. 53 (1988) 2111–2113. https://doi.org/10.1063/1.100292.
[19] D. Chen, Q. Lu, Y. Zhao, Laser-induced site-selective silver seeding on polyimide for electroless copper plating, Appl. Surf. Sci. 253 (2006) 1573–1580. https://doi.org/10.1016/j.apsusc.2006.02.039.
[20] M. Subramanian, A. Miaskowski, S.I. Jenkins, J. Lim, Remote manipulation of magnetic nanoparticles using magnetic field gradient to promote cancer cell death, Appl. Phys. A. 125 (2019). https://doi.org/doi:10.1007/s00339-019-2510-3.
[21] V.H.B. Ho, K.H. Müller, N.J. Darton, D.C. Darling, F. Farzaneh, N.K.H. Slater, Simple magnetic cell patterning using streptavidin paramagnetic particles, Exp. Biol. Med. 234 (2009) 332–341. https://doi.org/10.3181/0809-RM-273.
[22] G. Frasca, F. Gazeau, C. Wilhelm, Formation of a Three-Dimensional Multicellular Assembly Using Magnetic Patterning, Langmuir. 25 (2009) 2348–2354.
[23] Z. Yang, J. Wei, K. Gizynski, M.G. Song, B.A. Grzybowski, Interference-like patterns of static magnetic fields imprinted into polymer/nanoparticle composites, Nat. Commun. 8 (2017) 1–8. https://doi.org/10.1038/s41467-017-01861-1.
[24] S. Danilova, J.E. Graves, A.J. Cobley, Selective electroless metallization of non-conductive substrates enabled by a Fe<inf>3</inf>O<inf>4</inf>/Ag catalyst and a gradient magnetic field, Mater. Lett. 219 (2018). https://doi.org/10.1016/j.matlet.2018.02.062.
[25] S. Danilova, J.E. Graves, E. Pellicer, J. Sort, A.J. Cobley, Selective Metallization of Non-Conductive Materials by Patterning of Catalytic Particles and the Application of a Gradient Magnetic Field, ECS Trans. 85 (2018) 69–78. https://doi.org/10.1149/08504.0069ecst.
[26] S. Danilova, J.E. Graves, G.V.W. Cave, J. Sort, E. Pellicer, A.J. Cobley, Selective electroless plating on non-conductive materials by applying a gradient of magnetic field, Nov. Patterning Technol. Semicond. MEMS/NEMS MOEMS 2020. 11324 (2020) 1132412.
[27] B. Lv, Y. Xu, H. Tian, D. Wu, Y. Sun, Synthesis of Fe3O4SiO2Ag nanoparticles and its application in surface-enhanced Raman scattering, J. Solid State Chem. 183 (2010) 2968–2973. https://doi.org/10.1016/j.jssc.2010.10.001.
[28] H. Liang, H. Niu, P. Li, Z. Tao, C. Mao, J. Song, S. Zhang, Multifunctional Fe 3 O 4 @ C @ Ag hybrid nanoparticles : Aqueous solution preparation , characterization and photocatalytic activity, Mater. Res. Bull. 48 (2013) 2415–2419. https://doi.org/10.1016/j.materresbull.2013.02.066.
[29] Y. Chi, Q. Yuan, Y. Li, J. Tu, L. Zhao, N. Li, X. Li, Synthesis of Fe3O4@SiO2-Ag magnetic nanocomposite based on small-sized and highly dispersed silver nanoparticles for catalytic reduction of 4-nitrophenol, J. Colloid Interface Sci. 383 (2012) 96–102. https://doi.org/10.1016/j.jcis.2012.06.027.
[30] M.A. Y. Shacham-Diamand, V. Dubin, Electroless copper deposition for ULSI, Thin Solid Film. 262 (1995) 93–103.

[31] J.E.A.M. Van Den Meerakker, On the mechanism of electroless plating. I. Oxidation of formaldehyde at different electrode surfaces, J. Appl. Electrochem. 11 (1981) 387–393. https://doi.org/10.1007/BF00613959.
[32] I. Ohno, O. Wakabayashi, S. Haruyama, Anodic Oxidation of Reductants in Electroless Plating, J. Electrochem. Soc. 132 (1985) 2323. https://doi.org/10.1149/1.2113572.
[33] E. Steinhäuser, Potential low-cost palladium-alternatives for activating electroless copper deposition, Circuit World. 36 (2010) 4–8. https://doi.org/10.1108/03056121011066279.
[34] Y. Wang, N. Li, D. Li, S. Yu, C. Wang, A bio-inspired method to inkjet-printing copper pattern on polyimide substrate, Mater. Lett. 140 (2015) 127–130. https://doi.org/10.1016/j.matlet.2014.11.006.
[35] D.R. Lide, Handbook of Chemistry and Physics, National Institute of Standards and Technology, 2003.
[36] K. Ino, A. Ito, H. Honda, Cell patterning using Magnetite Nanoparticles and Magnetic force, Biotechnol. Bioeng. 97 (1996) 503–505. https://doi.org/10.1002/bit.
[37] Q. Cao, Z. Wang, B. Zhang, Y. Feng, S. Zhang, X. Han, L. Li, Targeting Behavior of Magnetic Particles Under Gradient Magnetic Fields Produced by Two Types of Permanent Magnets, IEEE Trans. Appl. Supercond. 26 (2016).
[38] K. Ino, M. Okochi, N. Konishi, M. Nakatochi, R. Imai, M. Shikida, A. Ito, H. Honda, Cell culture arrays using magnetic force-based cell patterning for dynamic single cell analysis, Lab Chip. 8 (2008) 134–142. https://doi.org/10.1039/B712330B.
[39] G. Hinds, F.E. Spada, J.M.D. Coey, T.R. Ni Mhiochain, M.E.G. Lyons, Magnetic Field Effects on Copper Electrolysis, J. Phys. Chem. B. 105 (2001) 9487–9502. https://doi.org/10.1021/jp010581u.

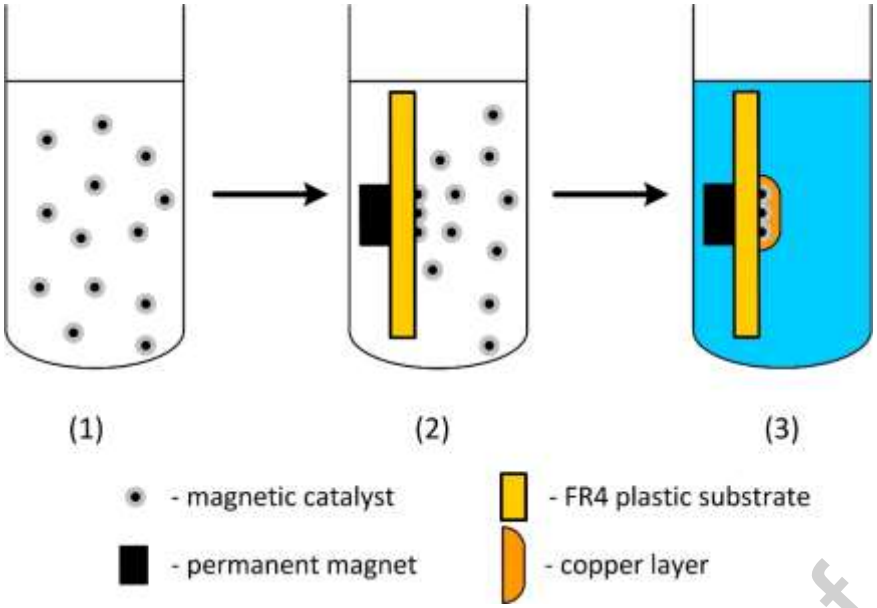

Figure 1. Schematic diagram of the SMMF process: (1) – dispersion of the magnetic particles; (2) – selective deposition of magnetic catalyst; (3) – electroless copper plating.

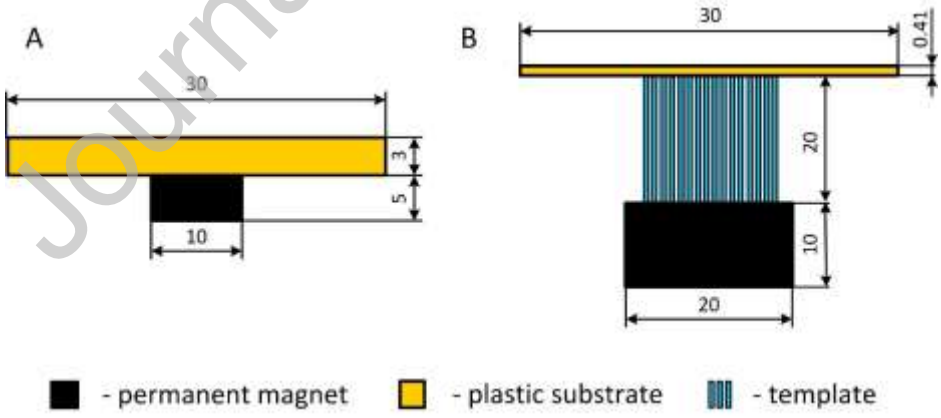

Figure 2. The configurations of plastic substrate, magnet and template used for the SMMF process during catalyst deposition and the electroless plating process: A – configuration 1, B – configuration 2. The main dimension are shown in mm, more details are provided in section 2.3.

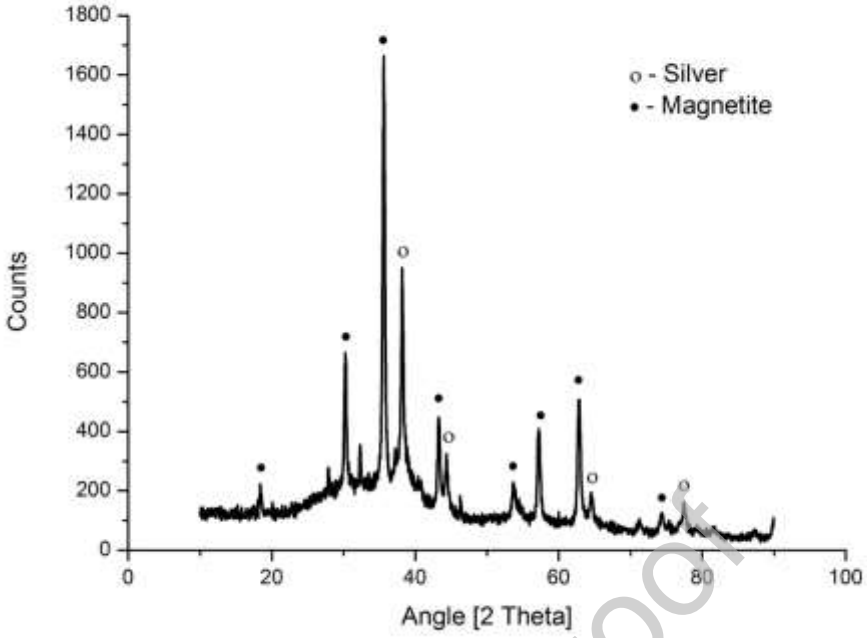

Figure 3. XRD pattern of composite magnetic catalyst particles.

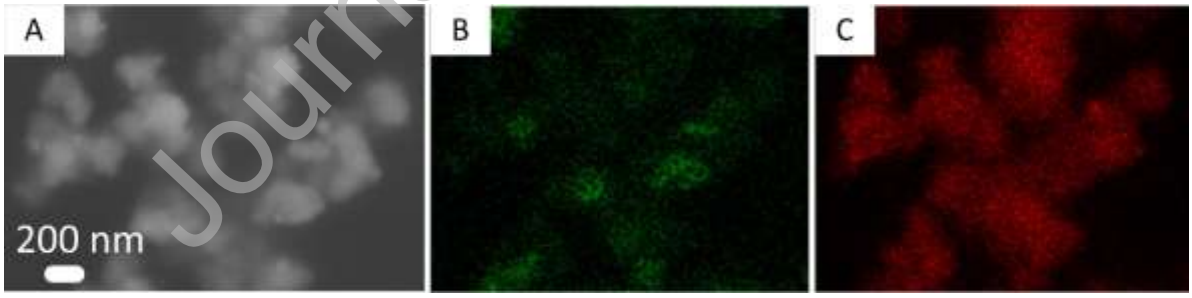

Figure 4. A – SEM image of the magnetic catalyst particles, B – EDX mapping of Fe within the sample, C – EDX mapping of Ag within the sample.

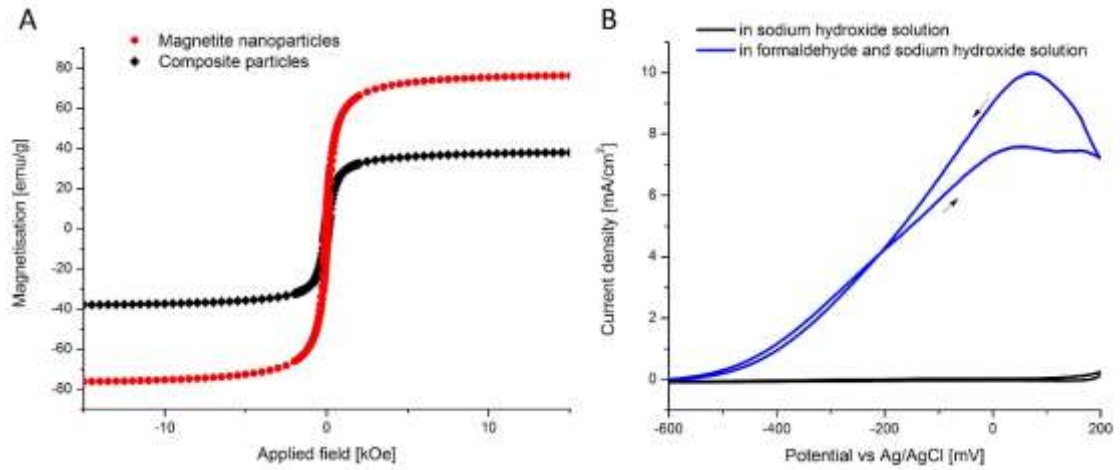

Figure 5. A – Magnetization curve of magnetic composite catalyst and precursor magnetite nanoparticles; B – results of the cyclic voltammetry experiment on the magnetic catalyst particles in sodium hydroxide solution with and without formaldehyde.

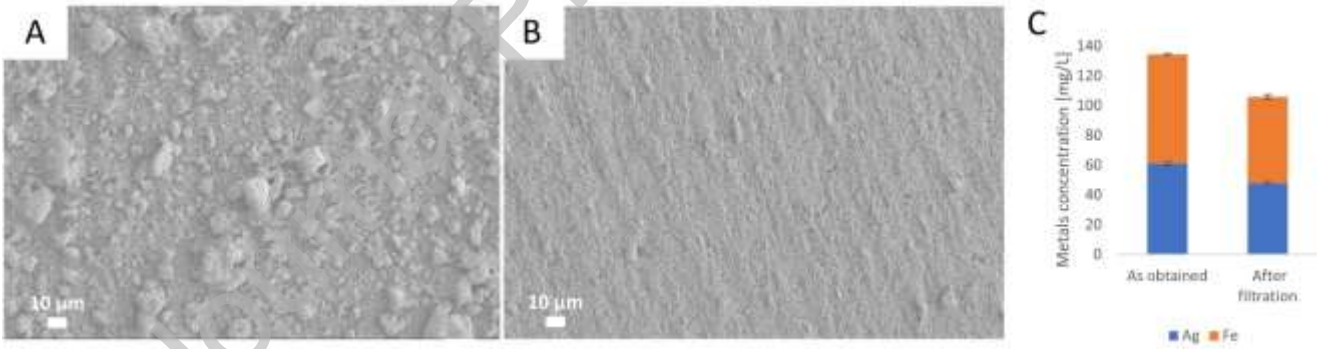

Figure 6. Magnetic catalyst particles deposited on the substrate surface by using configuration 1 from the dispersion A – before filtration, and B – after filtration. C - ICP measurement of Ag and Fe ion concentration in the dispersion of magnetic catalyst before and after filtration.

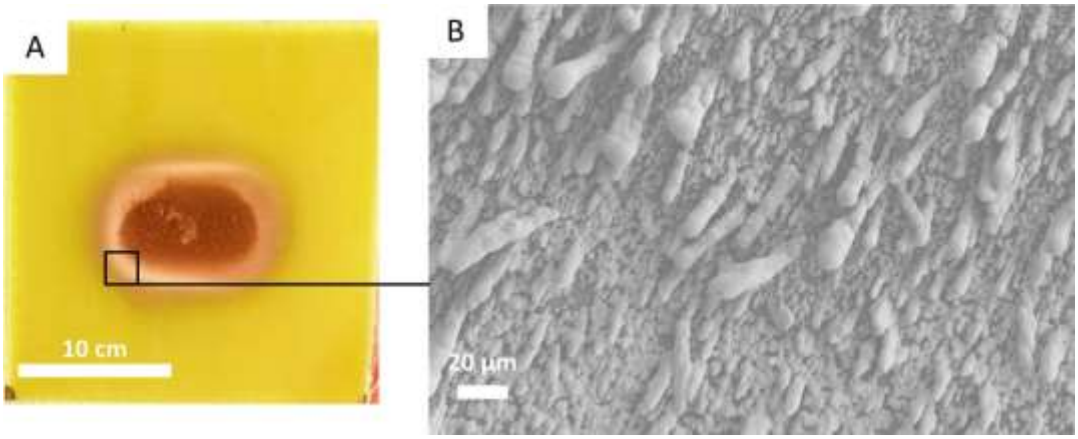

Figure 7. Selective copper plating on the substrate using the SMMF process in configuration 1. A – digital image, B – SEM image of the edge of the deposit.

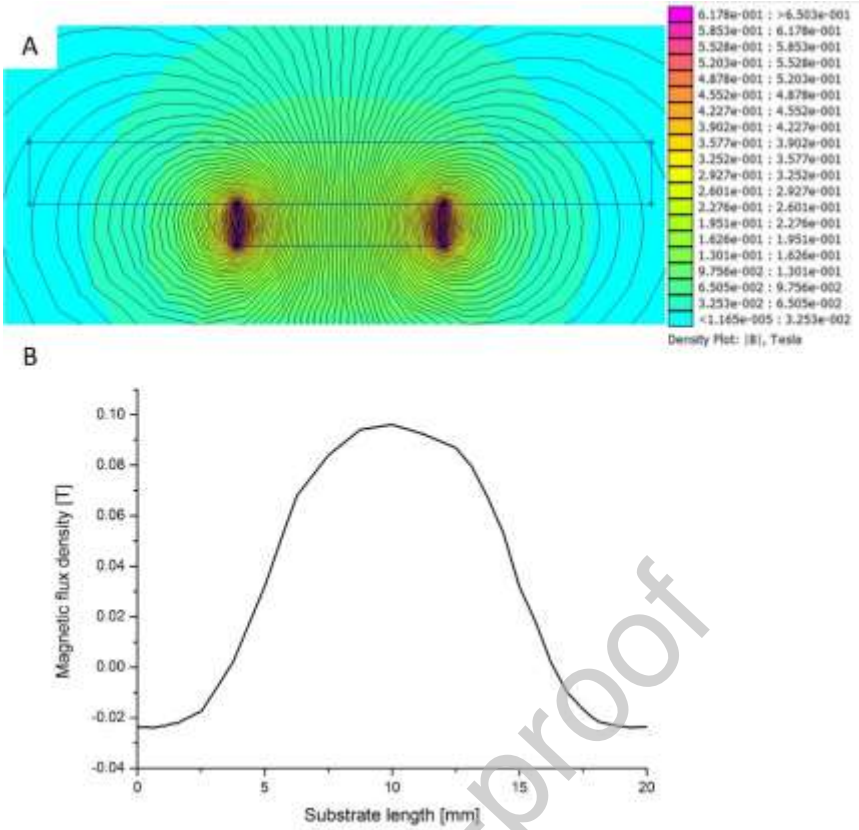

Figure 8. Simulation of magnetic flux density distribution in configuration 1 plotted using FEMM software, A – cross-section of the set-up, B – distribution of flux density across substrate upper surface.

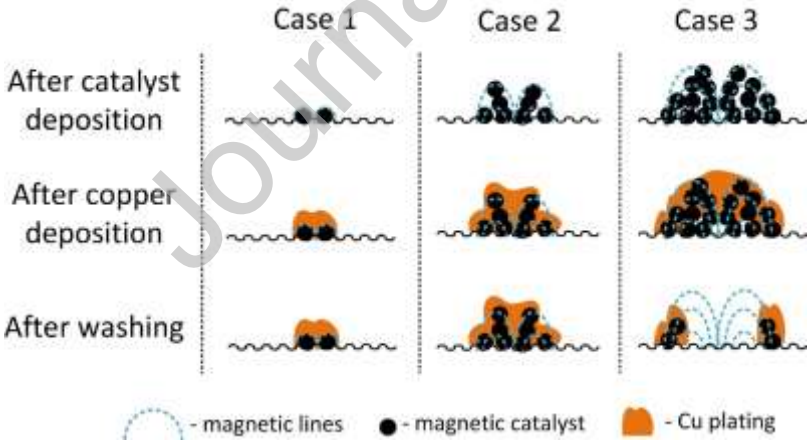

Figure 9. Schematic representation of the possible arrangement of catalyst on the substrate surface during the SMMF process and resultant electroless copper plating defects: case 1 – desirable distribution of the catalyst on the substrate surface, case 2 – needle-like arrangement of the catalyst which leads to needle-like copper plating, case 3 – overloading of the substrate surface with catalyst.

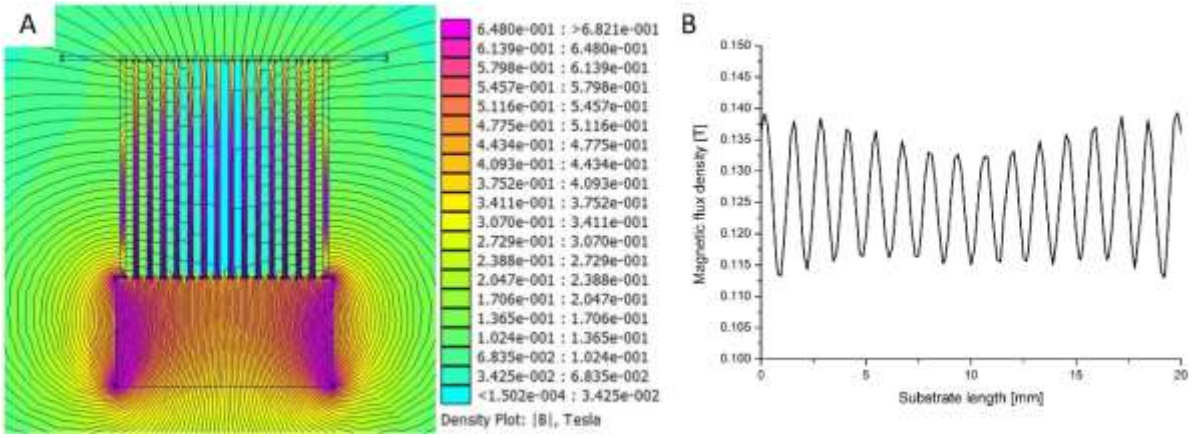

Figure 10. Simulation of magnetic flux density distribution in configuration 2 plotted using FEMM software, A – cross-section of the set-up, B – distribution of flux density across substrate upper surface.

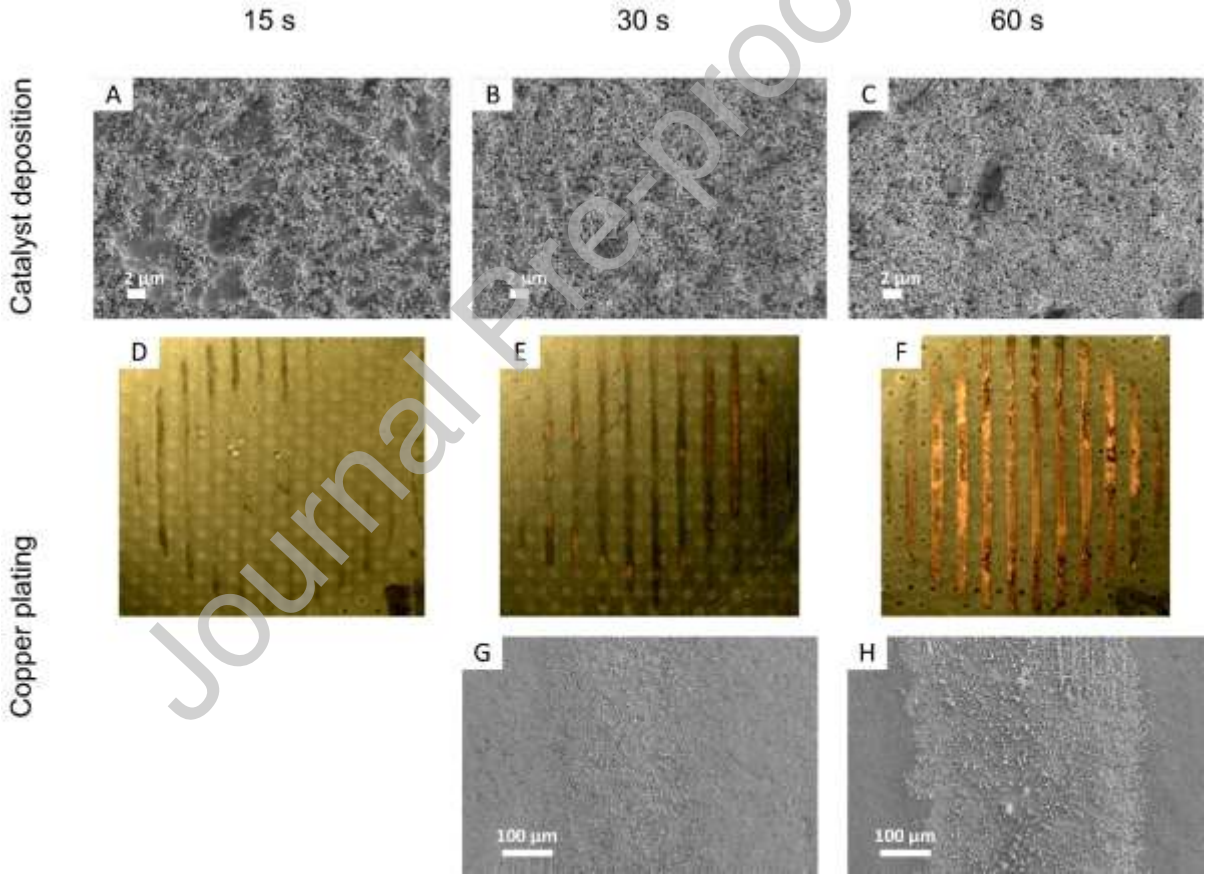

Figure 11. SEM images of magnetic composite catalyst (A-C) and digital (D-F) and SEM (G,H) images of subsequent electroless copper deposited via the SMMF process. Catalyst was deposited for 15 s (A, D), 30 s (B, E, G) and 60 s (C, F, H).

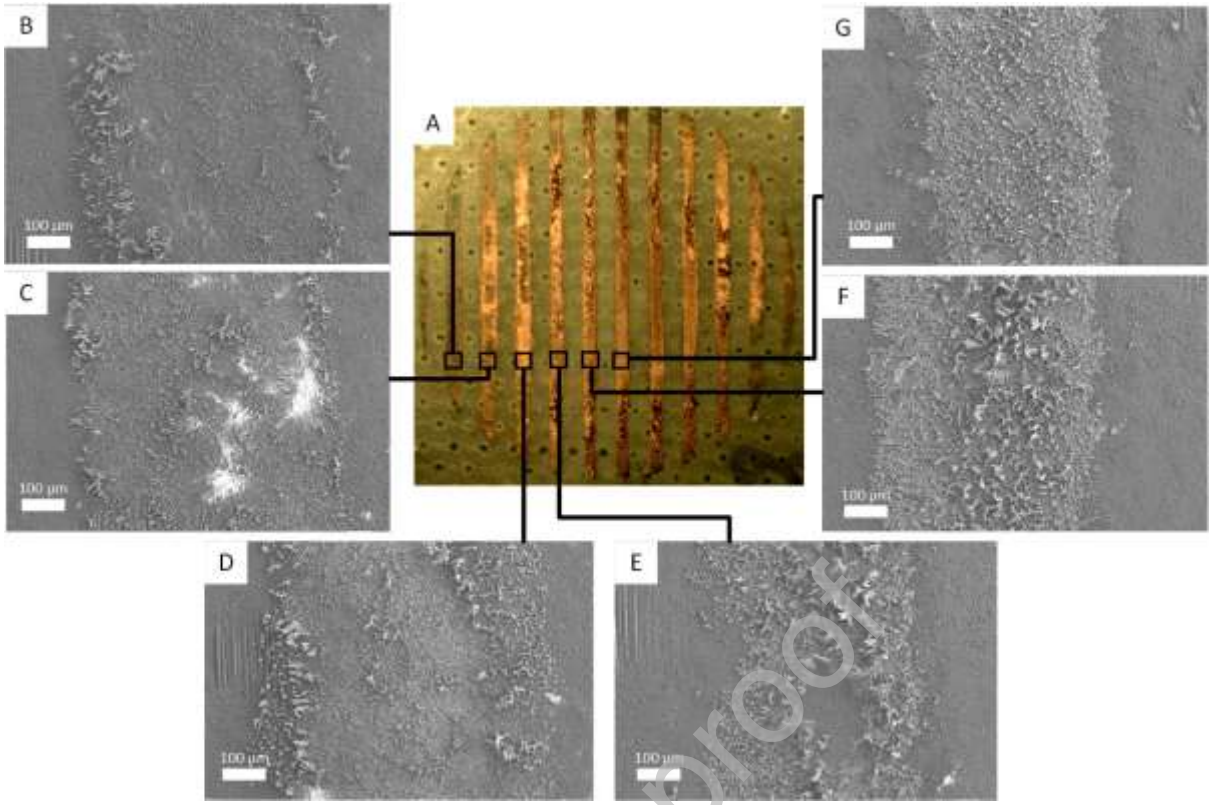

Figure 12. A - Digital image of electroless copper deposited using the SMMF process after 60 s of catalyst deposition with SEM images of the individual lines (A-F).

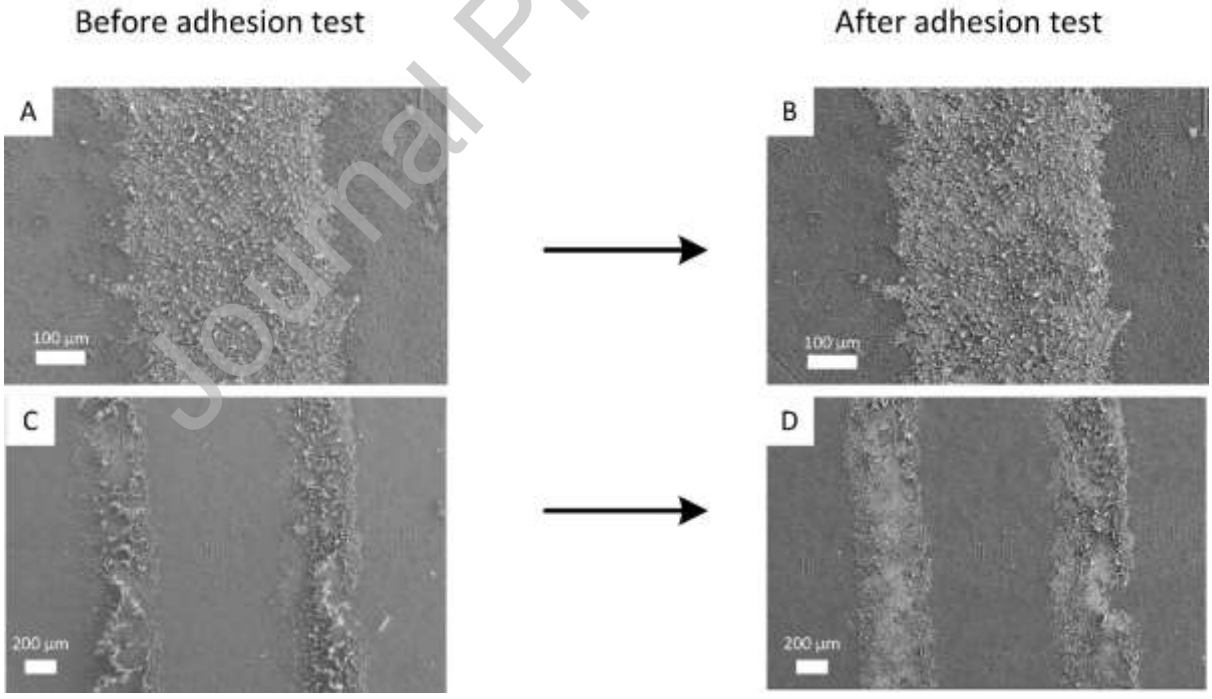

Figure 13. SEM images of electroless copper deposited using the SMMF process A, C – before adhesion tape test, B, D – after adhesion tape test.